Static solutions of Einstein's field equations for compact stellar objects

Omair Zubairi[1,2], Alexis Romero[2], and Fridolin Weber[2,3]

[1] Computational Science Research Center, San Diego State University, 5500 Campanile Drive, San Diego, CA 92182, USA

[2] Department of Physics, San Diego State University, 5500 Campanile Drive, San Diego, CA 92182, USA

[3] Center for Astrophysics and Space Sciences, University of California, San Diego, La Jolla, CA 92093, USA

E-mail: zubairi@rohan.sdsu.edu[1,2], romero14@rohan.sdsu[2], fweber@mail.sdsu.edu[2,3]

Abstract. In this work, we present two solutions of Einstein's field equations for compact stellar objects such as quark or neutron stars. Due to their unique stellar properties, these compact objects pose as excellent laboratories to study matter in the most extreme conditions. In part one of this paper, we solve Einstein's field equations modified for a finite value for the cosmological constant for spherically symmetric mass distributions. This solution has been presented in the literature before, but with inconsistent results. In part two, we examine the structure of deformed (non-spherical) compact objects. The stellar structure equations are derived and solved for in the limiting case of isotropic pressure and energy-density. We calculate stellar properties such as masses and radii along with pressure and density profiles for these deformed objects and investigate changes from the standard spherical models.

1. The Cosmological Constant and Compact Stars

In recent years, scientists have discovered that the expansion rate of the Universe is increasing rather than decreasing [1, 2]. This cosmic acceleration leads to an additional term in Einstein's field equation which is known as the cosmological constant. Albert Einstein originally introduced this term in 1916 as a modification of his field equation to achieve a stationary Universe, but quickly abandoned the concept after Hubble's discovery of the Universe expanding. This work explores the consequences of a non-vanishing cosmological constant for spherically symmetric mass distributions of compact stars such as quark or neutron stars.

In order to study compact stars, we must first investigate the stellar structure of these objects. The stellar properties of any compact object are dependent on the star's internal structure, which is described by the equation of state (EoS). Using Einstein's field equations, J. R. Oppenheimer and G. M. Volkoff [3] derived a differential equation using the work of R. C. Tolman [4] that describes the stellar structure of a compact object of isotropic material in hydrostatic equilibrium. This first order differential equation known as the Tolman-Oppenheimer-Volkoff (TOV) equation (Eq. (1)) is

$$\frac{dP}{dr} = -\frac{\varepsilon\left(1+\frac{P}{\varepsilon}\right) m\left(1+\frac{4\pi P r^3}{m}\right)}{r^2\left(1-\frac{2m}{r}\right)}\,, \tag{1}$$

where the natural units of $G = c = 1$. In Eq. (1) P is the pressure, ε is the energy-density, and m is the mass inside a spherical mass shell of radius r.

It has been suggested by a few authors [5, 6, 7] what form Eq. (1) should have with a modification of a cosmological constant. In previous work conducted by Reddy and Silbar,they suggest that only the numerator of Eq. (1) would change [7]; however, upon further inspection we find that this is not the only modification, but another term must be in the denominator. Papers from Ghezzi [6] and Vinayaraj and Kuriakose [5] show a modified TOV equation that includes a cosmological constant; however, we find that there are some inconsistencies with some of the terms in their TOV equation. In Section 1.1, we present the key equations and perform a derivation of the TOV equation from Einstein's field equation for a non-vanishing cosmological constant. For the entire step by step derivation, see [8]. In Section 1.3, solutions for compact stellar mass distributions (such as mass, radius, pressure and density profiles) are then obtained by the use of a simple relativistic quark equation of state (EoS).

1.1. Derivation of Modified TOV Equation

We start our calculations with the line element for a spherically symmetric mass distribution which has the form [9, 10]

$$ds^2 = \mathrm{e}^{\nu}dt^2 - \mathrm{e}^{\lambda}dr^2 - r^2d\theta^2 - r^2\sin^2(\theta)d\phi^2 \ , \tag{2}$$

where $\nu = \nu(r)$ and $\lambda = \lambda(r)$ are unknown metric functions. The non-vanishing components of the metric tensor in covariant form are given by

$$\begin{aligned} g_{tt} &= \mathrm{e}^{\nu} \ , \\ g_{rr} &= -\mathrm{e}^{\lambda} \ , \\ g_{\theta\theta} &= -r^2 \ , \\ g_{\phi\phi} &= -r^2\sin^2(\theta) \ , \end{aligned} \tag{3}$$

so that Eq. (2) can be written as

$$ds^2 = g_{\mu\nu}dx^{\mu}dx^{\nu} \ . \tag{4}$$

Due to spherical symmetry and time independence, the metric functions only have radial dependence. We start our calculations from Einstein's field equations in mixed representation given by

$$G^{\mu}_{\lambda} \equiv R^{\mu}_{\lambda} - \frac{1}{2}\delta^{\mu}_{\lambda}R + \Lambda\delta^{\mu}_{\lambda} = -8\pi T^{\mu}_{\lambda} \ , \tag{5}$$

where R^{μ}_{λ} is the Ricci tensor, R is the Ricci scalar, Λ is the cosmological constant, and T^{μ}_{λ} is the energy-momentum tensor which is given in terms of pressure P and the energy-density ε of the stellar matter [9, 10]

$$T^{\mu}_{\lambda} = (\varepsilon + P)\frac{dx_{\lambda}}{ds}\frac{dx^{\mu}}{ds} - \delta^{\mu}_{\lambda}P \ . \tag{6}$$

The energy-momentum tensor, (Eq. (6)) is for a (ideal) fluid with no viscosity and heat conduction.

Starting with the Einstein tensor, we calculate the t, r, θ, and ϕ components of the Einstein tensor and obtain expressions that take the form

$$\begin{aligned} G_t^t &\equiv R_t^t - \tfrac{1}{2}R + \Lambda &&= -T_t^t \ , \\ G_r^r &\equiv R_r^r - \tfrac{1}{2}R + \Lambda &&= -T_r^r \ , \\ G_\theta^\theta &\equiv R_\theta^\theta - \tfrac{1}{2}R + \Lambda &&= -T_\theta^\theta \ , \\ G_\phi^\phi &\equiv R_\phi^\phi - \tfrac{1}{2}R + \Lambda &&= -T_\phi^\phi \ . \end{aligned} \tag{7}$$

Once we have determined the left hand side terms of Eq. (7), we will equate those terms with the right hand side respectively.

We calculate the components of the Ricci tensor to be [8]

$$R_t^t = \left[-\frac{\nu'^2}{4} + \frac{\nu'\lambda'}{4} - \frac{\nu''}{2} - \frac{\nu'}{2} \right] \mathrm{e}^{-\lambda} \ , \tag{8}$$

and

$$R_r^r = -\left[\frac{\nu'^2}{4} - \frac{\lambda'\nu'}{4} - \frac{\lambda'}{r} - \frac{\nu''}{2} \right] \mathrm{e}^{-\lambda} \ , \tag{9}$$

along with the Ricci scalar given by

$$\begin{aligned} R &= g^{\mu\nu} R_{\mu\nu} \\ &= \mathrm{e}^{-\lambda} \left[-\frac{\nu'^2}{2} - \nu'' + \frac{\nu'\lambda'}{2} - \frac{2\nu'}{r} + \frac{2\lambda'}{r} - \frac{2}{r^2} \right] + \frac{2}{r^2} \ . \end{aligned} \tag{10}$$

Substituting Eqs. (8), (9), and (10) into Eq. (7), we calculate the components of the Einstein tensor to be [8]

$$\begin{aligned} G_t^t &= \mathrm{e}^{-\lambda} \left(-\frac{\lambda'}{r} + \frac{1}{r^2} \right) - \frac{1}{r^2} + \Lambda \ , \\ G_r^r &= \mathrm{e}^{-\lambda} \left(\frac{\nu'}{r} + \frac{1}{r^2} \right) - \frac{1}{r^2} + \Lambda \ , \\ G_\theta^\theta &= G_\phi^\phi \ . \end{aligned} \tag{11}$$

Equating Eq. (6) to Eq. (11), we obtain

$$\begin{aligned} 8\pi\varepsilon &= \mathrm{e}^{-\lambda} \left(\frac{\lambda'}{r} - \frac{1}{r^2} \right) + \frac{1}{r^2} - \Lambda \ , \\ 8\pi P &= \mathrm{e}^{-\lambda} \left(\frac{\nu'}{r} + \frac{1}{r^2} \right) - \frac{1}{r^2} + \Lambda \ . \end{aligned} \tag{12}$$

Using the gravitational mass,

$$m(r) = 4\pi \int_0^r \varepsilon(r') r'^2 \, dr' \ , \tag{13}$$

and other mathematical means [8], we calculate the $r-$component of Eq. (2) to be

$$e^{-\lambda(r)} = 1 - \frac{2m(r)}{r} - \frac{\Lambda r^2}{3} \ . \tag{14}$$

Adding the expressions given in Eq. (12) and using Eq. (14), along with other mathematical methods [8], our modified TOV equation with a non-vanishing cosmological constant is

$$\frac{dP}{dr} = -\frac{\varepsilon\left(1+\frac{P}{\varepsilon}\right) m\left(1+\frac{4\pi P r^3}{m} - \frac{\Lambda r^3}{3m}\right)}{r^2\left(1-\frac{2m}{r}-\frac{\Lambda r^2}{3}\right)} \ , \tag{15}$$

where the units of Λ are given in MeV/fm^3. From Eq. (15), one can easily see if Λ is small ($\approx 10^{-41}$) [11], we will get no contributions for the bulk properties. Λ would have to be on the order of nuclear density scales (140 MeV/fm^3) to see any significant changes in mass and radius.

We can solve Eq. (15) for a given equation of state (EoS) model and produce stellar properties such as masses, radii, pressure and density profiles, along with the gravitational redshift. Section 1.2 briefly describes the EoS model used in this work.

1.2. Equation of State

For simplicity, we use the well known EoS of a relativistic gas of de-confined quarks also known as the MIT bag model [12, 13, 14]. This EoS model will allow us to mimic stellar properties such as masses and radii of neutron stars. In this model the pressure P^f, (where f are the quark flavors $f = u, d, s$) of the individual quarks are contained in a bag which is counterbalanced by the total external bag pressure, B, and will have the form

$$P + B = \sum_f P^f \ . \tag{16}$$

The total energy-density ε of the quarks inside the bag is is given by

$$\varepsilon = \sum_f \varepsilon^f + B \ , \tag{17}$$

where $\varepsilon^f = 3P^f$ denote the contributions that the individual quarks have on the total energy density. The term B is the known as the bag constant. The EoS is then obtained which has the form [12, 13, 15, 16]

$$P = \frac{\varepsilon - 4B}{3} \ . \tag{18}$$

One can see from Eq. (18) that the pressure becomes zero when $\varepsilon = 4B$. The mass contained in a spherical shell of radius r is given by Eq. (13). The total mass M of a stellar configuration is therefore given by $M = m(R)$, where R denotes the radius of the stellar mass distribution, which is defined by $P(r = R) = 0$. By using Eqs. (13) and (18), we solve Eq. (15) and produce stellar properties such as mass, radius, pressure and density profiles.

1.3. Results

Solving Eq. (15) in combination with Eq. (18) and inputting different values of Λ, we calculate the masses and radii of stellar configurations made of a relativistic quark gas (quark stars) [8]. Figures 1 and 2 show the mass-radius relationships for these objects.

Figures 1 and 2 show the mass-radius relationships of stellar sequences for negative and positive values of Λ respectively. We see that if $\Lambda = 0$ the maximum-mass is approximately $2M_\odot$, where $M_\odot$ denotes the mass of the sun (2.0×10^{30} kg). This is in agreement with known

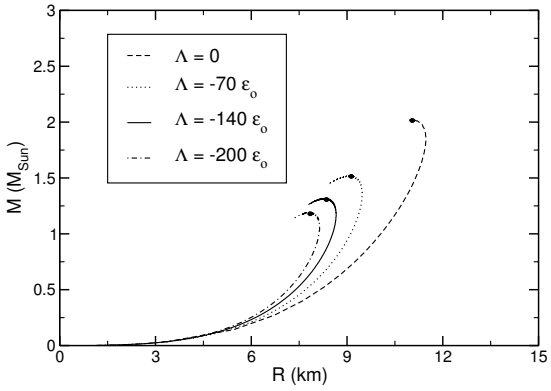

Figure 1. Mass-radius relationship for negative values of the cosmological constant Λ. (ε_0 denotes the energy-density of nuclear matter (140 MeV/fm^3).) The solid dots on each curve represent the maximum-mass star for each stellar sequence.

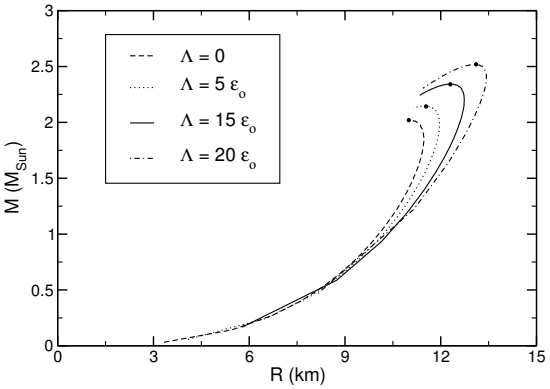

Figure 2. Mass-radius relationship for positive values of the cosmological constant Λ. (ε_0 denotes the energy-density of nuclear matter (140 MeV/fm^3).) The solid dots on each curve represent the maximum-mass star for each stellar sequence.

results from the literature [14, 15, 16, 17, 18, 19, 20]. If Λ becomes negative, we see that the star's mass and radius decrease. By inputting positive values for Λ, we get the opposite effect as shown in figure. 1.

Next, we calculate the pressure and density profiles of the maximum-mass objects shown in figures 1 and 2 [8]. The pressure profiles for each maximum mass stars are shown in figures 3 and 4. As it is shown in figures 3 and 4, the pressure becomes zero at the surface, which is in agreement with our boundary conditions.

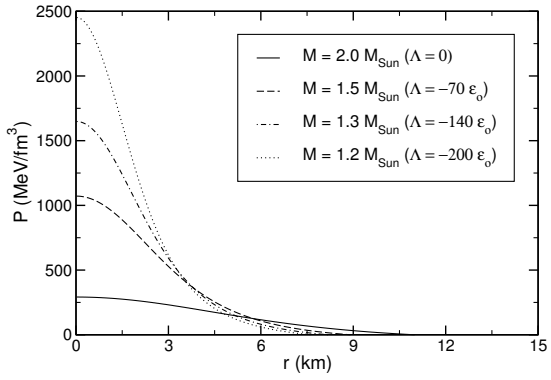

Figure 3. Pressure profiles for the maximum masses shown in figure 1. These profiles are for negative Λ values.

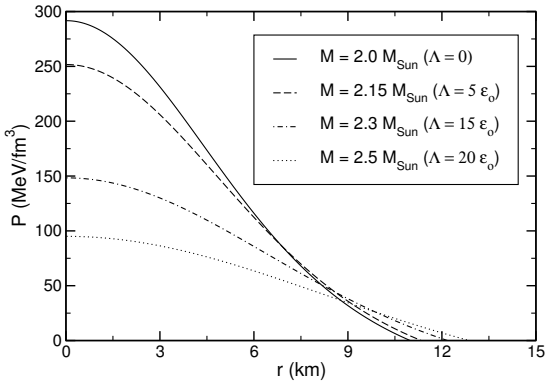

Figure 4. Pressure profiles for the maximum masses shown in figure 2. These profiles are for positive Λ values.

Next, we show the density profiles for each maximum mass in figures 1 and 2. The results are shown in figures 5 and 6. As one can see, the energy-density approaches to $4B$ as dictated by our EoS (Eq. (18)) for each maximum mass star.

From our results shown in figures 1 and 2, we have calculated the masses and radii of compact stars using a quark EoS. Since we now have numerical values for the total mass and radius, we

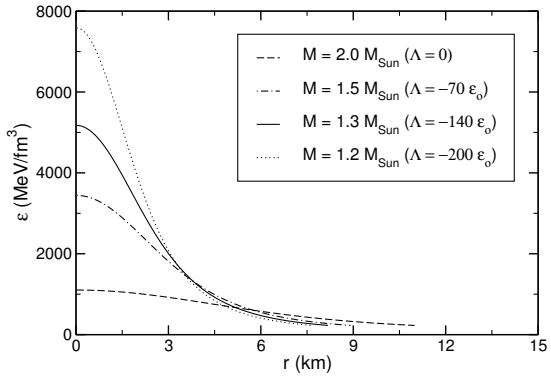

Figure 5. Energy-Density profiles for the maximum mass objects shown in figure 1.

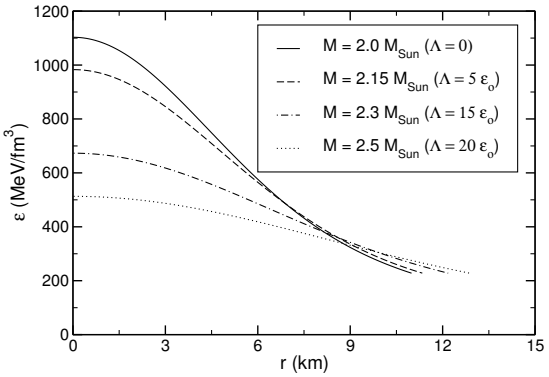

Figure 6. Energy-Density profiles for the maximum mass objects shown in figure 2.

can also calculate the gravitational redshift of these objects. The gravitational redshift is given by [9]

$$z = \frac{1}{\sqrt{1 - \frac{2M}{R}}} - 1 \ , \tag{19}$$

where, M and R are the mass and radius of a given stellar object. By using masses and radii that are associated with specific cosmological constant values and by Eq. (19), we calculate the gravitational redshift. The results are given in figure 7.

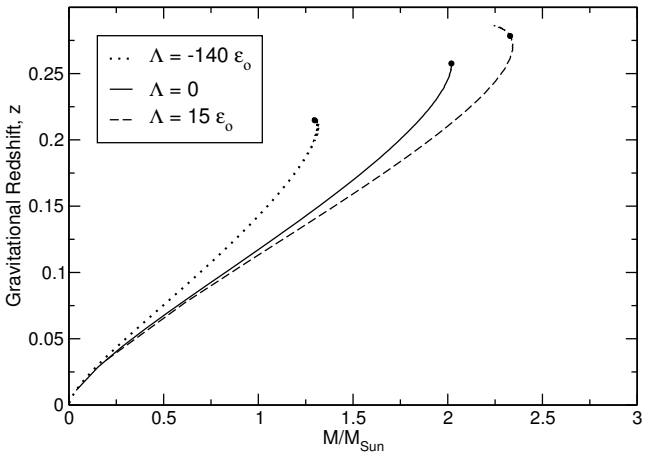

Figure 7. Gravitational redshift as a function of stellar mass for selected Λ values.

From Eq. (19), the limit of the ratio of mass and radius is less then 8/9 as described in [9] for any compact object satisfying the TOV equation. This limit will then yield a gravitational redshift of $z < 2$.

1.4. Conclusions

This work on the cosmological constant and compact stars consists in performing a derivation of the Tolman-Oppenheimer-Volkoff (TOV) equation modified for the cosmological constant Λ.

The form of this equation and solution has been stated in the literature by a few authors [5, 6, 7] already, however with disagreeing results and conclusions.

In order to investigate the role of the cosmological constant for compact objects, we have solved the modified TOV equation for mass distributions consisting of a relativistic quark gas [8]. We have obtained stellar properties such as mass, radius, pressure and density profiles along with gravitational redshifts [8] for a range of different Λ values. It follows from figures 1 through 6 that the stellar properties of compact objects in our Universe, where Λ is very small $\left(\Lambda{\approx}10^{-41}\mathrm{MeV/fm}^3\right)$ [9, 11, 21] do not depend on the cosmological constant, in contrast to claims expressed in the literature [5].

2. Non Spherical Stellar Models of Compact Stars

Conventionally, the structure of compact stellar objects such as neutron or quark stars are modeled with the assumption that they are perfect spheres. However, due to high magnetic fields up around 10^{18} G, certain classes of compact stars [22] (such as magnetars and neutron stars containing cores of color-superconducting quark matter) are expected to be deformed (non-spherical) making them ob-longed spheroids. In this part of our paper, we seek to investigate the stellar properties of deformed compact stars in the framework of general relativity. Using a metric that describes a non-spherical mass distribution, we derive the stellar structure equations of these non-spherical objects. We then calculate stellar properties such as mass and radii along with density and pressure profiles and investigate any changes from the standard spherical models.

2.1. Non-Spherical Symmetry

In order to understand how the deformation will impact the stellar configurations, we must first take a look at the symmetry of these objects. We begin with a standard spherically symmetric object of radius r.

We introduce a deformation constant γ and normalize it when $\gamma = 1$ to be a perfect sphere. The deformation of the stellar objects can have two outcomes: (1) Equatorial deformation (oblate spheroid) (2) polar deformation (prolate spheroid). In terms of γ the deformation can be defined as $\gamma < 1$, for equatorial deformation or $\gamma > 1$, for polar deformation.

For both cases, we are assuming axial symmetry (see figures 8 and 9)–meaning the axis of symmetry will be along the polar axis. The equatorial radii lie in the x-y plane of the star, while the polar radius z is orthogonal to the x-y plane. Hence, we only have to consider two distinct radii. Having our symmetry laid out in this fashion allows us now to derive the stellar structure equations that will govern the stellar properties of deformed compact stars.

2.2. Stellar Structure Equations

Since we are dealing with non-spherical symmetry as mentioned in section 2.1, we begin our calculations with an axial-symmetric metric in non-spherical coordinates given by [23, 25]

$$ds^2 = \mathrm{e}^{2\Phi}dt^2 - \mathrm{e}^{-2\Phi}\left[\mathrm{e}^{2\Lambda}\left(dr^2 + dz^2\right) + r^2 d\phi^2\right] \ , \tag{20}$$

where t is the time component, and r, z, and ϕ are the spatial components. Having this extra spatial dz component implies our calculations to be in 2-Dimensions. To simplify this scenario and as a first step towards this work, we parameterize the z-component in terms of γ and the radial component. This will allow two important facets:

(i) Use an EoS in the *limiting* case of isotropic pressure and density.
(ii) Still maintain deformation structure.

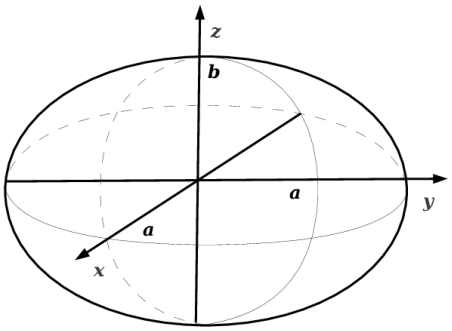

Figure 8. Oblate spheroid ($\gamma < 1$) with radii a and b.

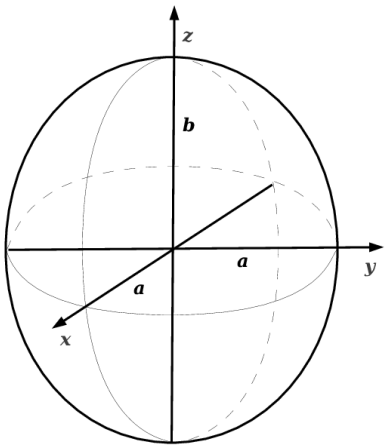

Figure 9. Prolate spheroid ($\gamma > 1$) with radii a and b.

Maintaining the deformation structure will allow us to examine how the mass and radii change due to the deformity. We begin with the examination of the components of the metric, specifically the components of this metric given in terms of [25]

$$\begin{aligned} \mathrm{e}^{2\Phi} &= \left[\frac{k_1+k_2-2m}{k_1+k_2+2m}\right]^{\gamma} , \\ \mathrm{e}^{2\Lambda} &= \left[\frac{(k_1+k_2+2m)\,(k_1+k_2-2m)}{4k_1k_2}\right]^{\gamma^2} , \end{aligned} \tag{21}$$

where

$$\begin{aligned} k_1 &= \sqrt{r^2+(z-m)^2} , \\ k_2 &= \sqrt{r^2+(z+m)^2} . \end{aligned} \tag{22}$$

Hence, the components of this metric are given in terms of equatorial radius r, polar radius z, along with the mass m inside a mass shell.

In the case where $\gamma = 1$, we obtain the metric for a spherically symmetric object of the form [25, 26]

$$ds^2 = Adt^2 - A^{-1}\left[Bdr^2 + Cd\theta^2 + \left(r^2-2mr\right)\sin^2(\theta)d\phi^2\right] = g_{\mu\nu}dx^{\mu}dx^{\nu} , \tag{23}$$

where

$$A = \left(1 - \frac{2m}{r}\right)^{\gamma} \ ,$$
$$B = \left(\frac{r^2 - 2mr}{r^2 - 2mr + m^2\sin^2(\theta)}\right)^{\gamma^2 - 1} \ ,$$
$$C = \frac{\left(r^2 - 2mr\right)^{\gamma^2}}{\left(r^2 - 2mr + m^2\sin^2(\theta)\right)^{\gamma^2 - 1}} \ . \tag{24}$$

Hence, Eq. (23) is now given in terms of our deformation constant and is parameterized. Using Eq. (23) along with other mathematical means [24] we solve Einstein's equations for $\Lambda = 0$, (Eqs. (5) and (6)) and arrive at the stellar structure equation of hydrostatic equilibrium for a deformed compact star

$$\frac{dP}{dr} = -\frac{(\epsilon + P)\left[\frac{1}{2}r + 4\pi r^3 P - \frac{1}{2}r\left(1 - \frac{2m}{r}\right)^{\gamma}\right]}{\left[r^2\left(1 - \frac{2m}{r}\right)^{\gamma}\right]} \ . \tag{25}$$

Eq. (25) describes how the pressure behaves inside a deformed compact star. In the limiting case when $\gamma = 1$, we will obtain Eq. (1) for hydrostatic equilibrium.

The total mass of a deformed compact star is given by $M = m(R)$, where R denotes the radius of the star given by $P(r = R) = 0$.

Since Eq. (25) is governed by a deformation constant (γ), the stellar mass must also be governed by the same constant and will have the form [25, 26]

$$M = \gamma m \ . \tag{26}$$

Hence, we utilize a parameterization for Eq. (26). Once we have our mass parameterized in terms of γ, we can then use an EoS model and calculate stellar properties of a deformed compact star.

2.3. Parameterization

We begin our parameterization by considering the volume of a sphere given by

$$V = \frac{4}{3}\pi r^3 \ , \tag{27}$$

where r is the radius of the sphere. However, in our case, we have two distinct radii as shown in figures 8 and 9 and hence, the volume of these oblate or prolate spheroids is given by

$$V = \frac{4}{3}\pi r^2 z \ , \tag{28}$$

where r is the equatorial radius and z is the polar radius. We can parameterize the polar radius by $z = \gamma r$ to give us

$$V = \frac{4}{3}\pi r^3 \gamma \ , \tag{29}$$

and therefore, our mass will now become

$$\frac{dm}{dr} = 4\epsilon\pi r^2 \gamma \ . \tag{30}$$

Having Eqs. (25) and (30) parameterized in terms of γ, we now solve these two coupled equations with the use of an EoS of relativistic quark gas as described in section 1.2.

2.4. Results

We first calculate the mass and radii of deformed objects which are parameterized by the deformation constant γ. The results are shown in figures 10 and 11.

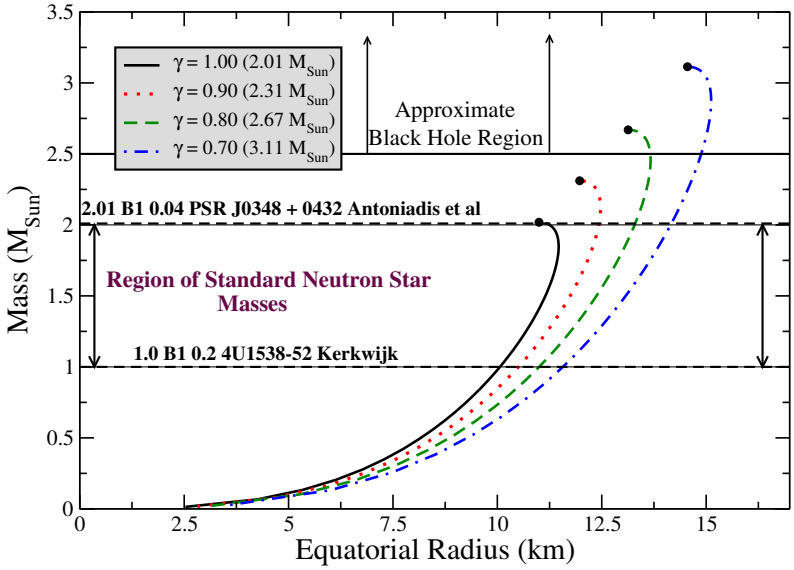

Figure 10. (Color online) Mass vs. equatorial radius for values of $\gamma < 1$. The dots on each curve represent the maximum mass star for each stellar sequence.

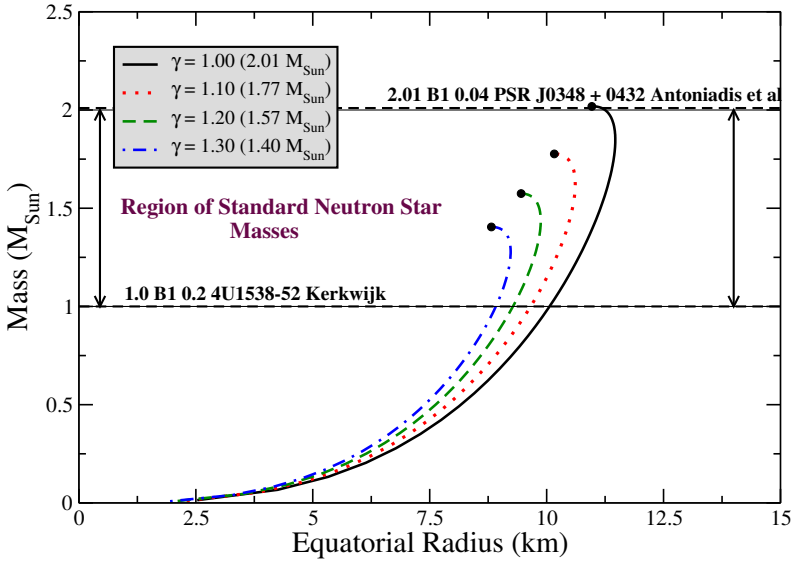

Figure 11. (Color online) Mass vs. equatorial radius for values of $\gamma > 1$. The dots on each curve represent the maximum mass star for each stellar sequence.

From figure 10, we see for the spherical case ($\gamma = 1$), we get a mass on the order of about 2 $M_\odot$ and an equatorial radius of about 10 km. However, if decrease γ by a mere 10 %, we get a 15 % increase in mass and an increase in equatorial radius by a few kilometers. A greater equatorial radius means a smaller polar radius, leading to an oblate compact star. If we continue to change γ, we see that the mass keeps increasing. However, this is not the case for when $\gamma > 1$. As shown in figure 11, if we increase γ by 10 % we get a 12 % decrease in mass and a decrease in equatorial radius. A smaller equatorial radii will result in a larger polar radius and thus we will have deformation in the polar direction leading to a prolate spheroid.

The change in mass due to the geometry of the deformation is interesting. From our results in figures 10 and 11, we can conclude that the deformation does change the mass of the compact star by a significant amount. The images in figure 12 show the total deformation for the maximum masses in figure 10.

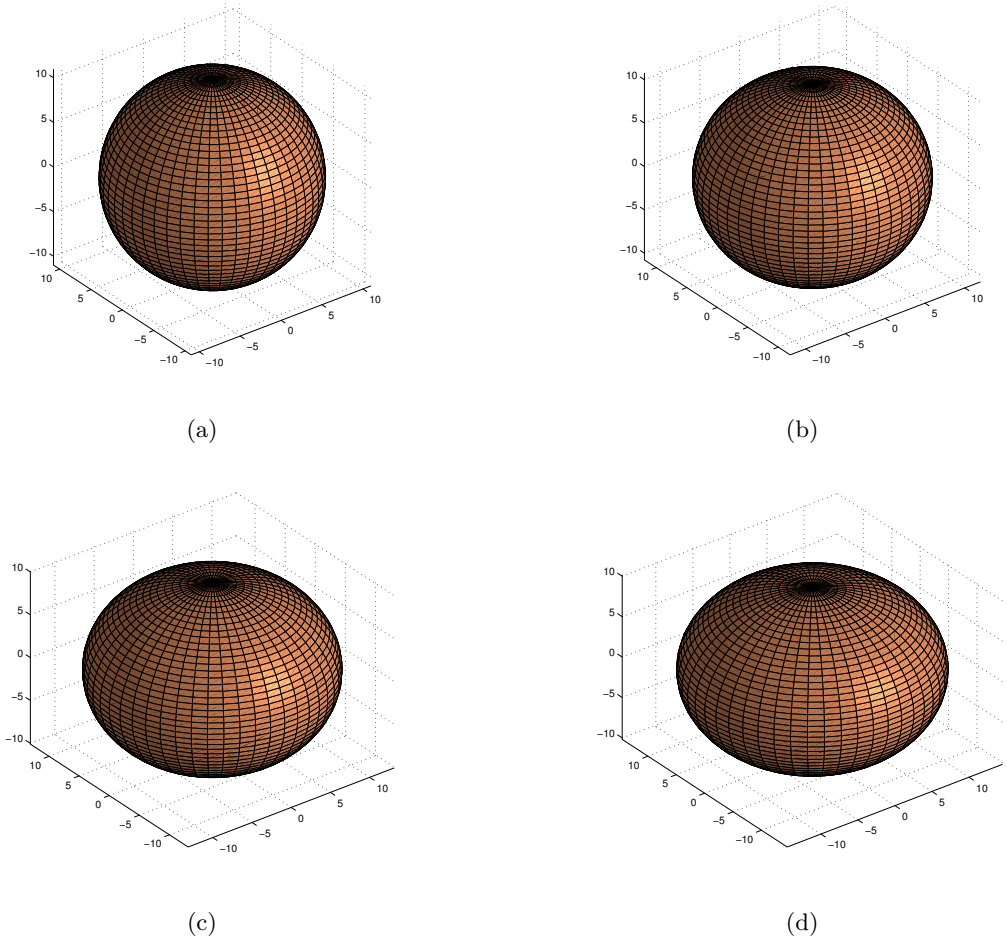

(a) (b)

(c) (d)

Figure 12. Shapes of the maximum mass stars given in figure 10. (a) $\gamma = 1.00$, M=2.01 $M_\odot$, (b) $\gamma = 0.90$, M=2.32 $M_\odot$, (c) $\gamma = 0.80$, M=2.67 $M_\odot$, (d) $\gamma = 0.70$, M=3.01 $M_\odot$

We next look at the prolate case for various values of our deformation constant γ. The images in figure 13 show the total deformation for the maximum masses in figure 11.

Since we have obtained stellar properties such as mass and radius the next step is to look at the pressure and density profiles associated with the maximum masses shown in figures 10 and 11. We calculate the pressure and density profiles in both the equatorial and polar radii for

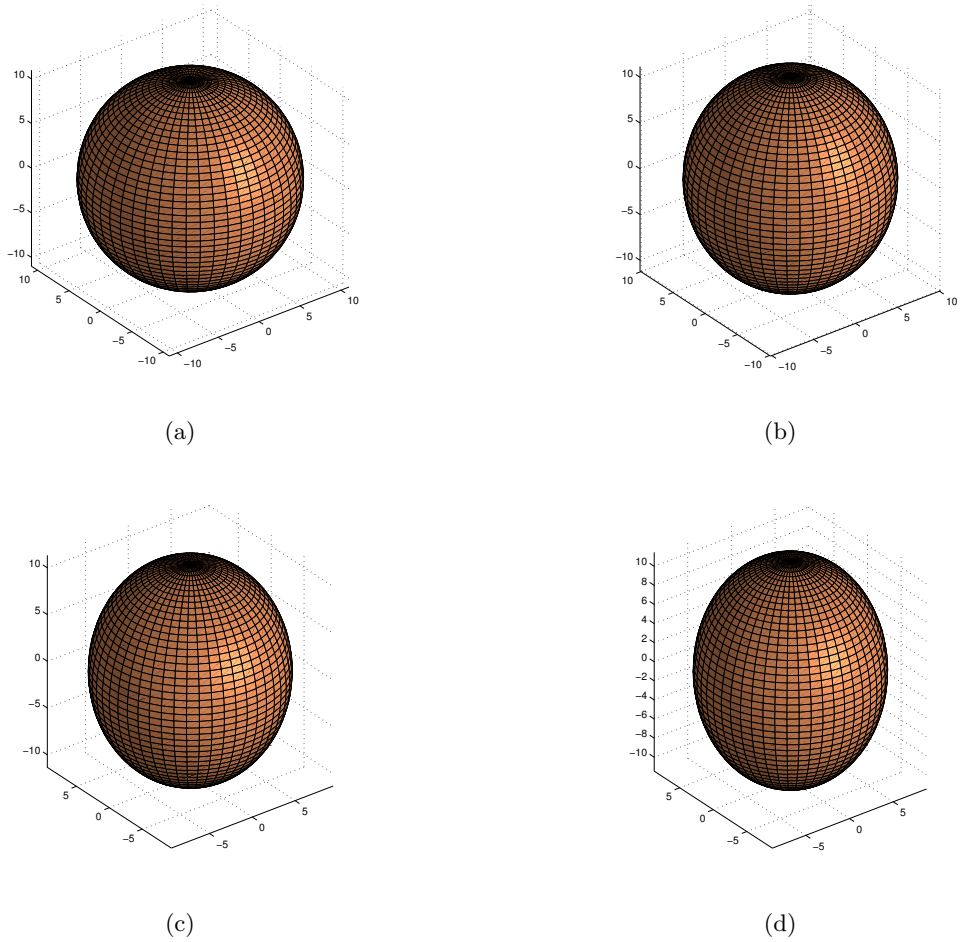

(a) (b)

(c) (d)

Figure 13. Shapes of the maximum mass stars given in figure 11. (a) $\gamma = 1.00$, M=2.01 $M_\odot$, (b) $\gamma = 1.10$, M=1.77 $M_\odot$, (c) $\gamma = 1.20$, M=1.57 $M_\odot$, (d) $\gamma = 1.30$, M=1.40 $M_\odot$

these maximum masses. The outcome is shown in figures 14 and 15, respectively.

From our results from figures 10 and 11, we see the that mass does change as we deformed the object either in the equatorial or polar directions. Since we have numerical values for the mass and radii, we can also investigate the gravitational redshift of these objects. However, since our metric is given in terms of γ, we must derive an expression of gravitational redshift which will relate stellar properties such as mass and radii in terms of γ.

We begin our redshift calculation with an examination of the components of the metric described by Eq. (23), in particular the $t-$component $g_{tt} = g_{00}$ is given by

$$g_{00} = \left(1 - \frac{2M}{R}\right)^{\gamma} , \tag{31}$$

where M and R represent the total mass and equatorial radii, along with our deformation constant γ.

Consider an idealized situation in which a photon is emitted from the surface of a star and travels through a gravitational field towards an observer located at infinity. The time interval dx^0 for this photon leaving the surface of the star is then given by [9]

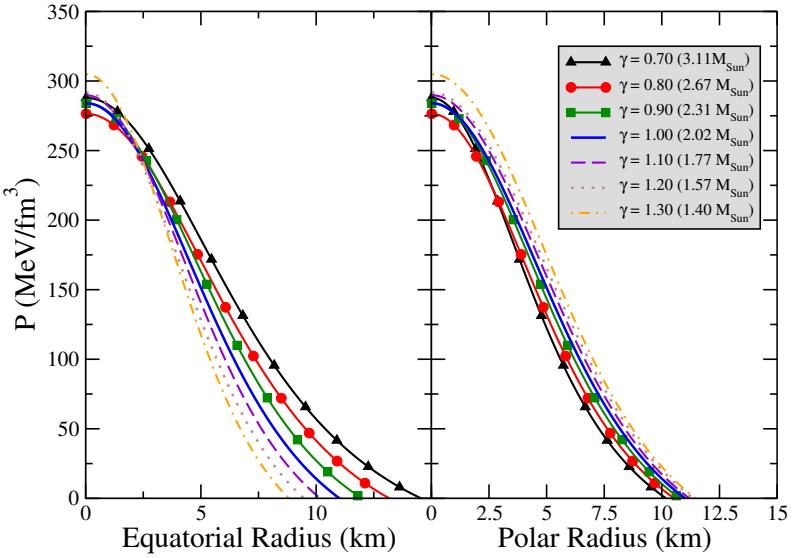

Figure 14. (Color online) Pressure profiles for the maximum mass stars shown in figures 10 and 11. All pressure profiles becomes zero for both the equatorial and polar radii as dictated by our boundary conditions.

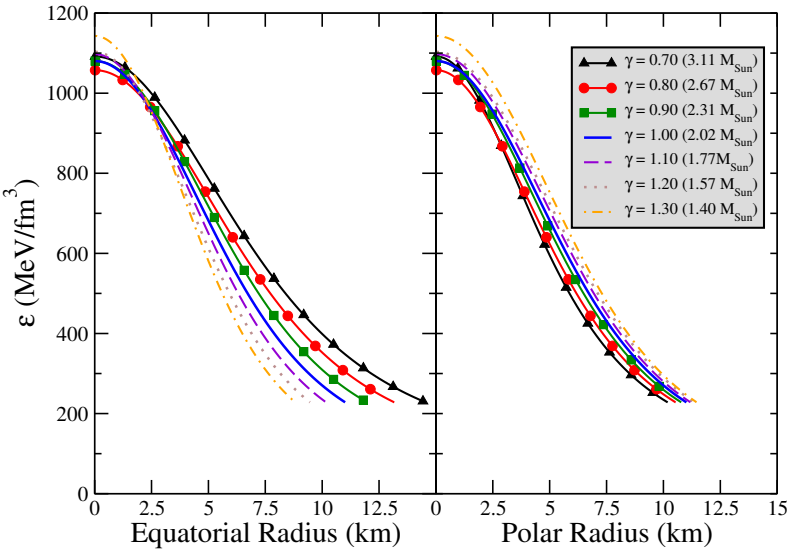

Figure 15. (Color online) Density profiles for the maximum mass stars shown in figures 10 and 11. As one can see, the density approaches to $4B$ as dictated by our EoS for the equatorial and polar radii.

$$d\tau_a = \sqrt{g_{00}(R)}dx^0 \ . \tag{32}$$

If we assume that light propagates in a radial direction in a static field, the time interval $d\tau^2$ is then described by

$$d\tau^2 = g_{00}(r)dt^2 - g_{11}(r)dr^2 = 0 \ . \tag{33}$$

Integrating Eq. (33), we find the constant time interval for each wave crest to travel from R to infinity to be

$$\Delta t = t_\infty - t_R = \int_R^\infty \left(\frac{g_{11}(r)}{g_{00}(r)}\right)^{1/2} dr \ , \tag{34}$$

where an observer located at ∞ will measure the proper time between the crests arriving from the star to be

$$d\tau_{a'} = \sqrt{g_{00}(\infty)}dx^0 \ . \tag{35}$$

If we consider an emission of a photon from ∞ toward the star, and we let the event be denoted by x'^μ. Then the equation that governs the coordinate time interval dx'^0 will be given by [9]

$$d\tau_a = \sqrt{g_{00}(\infty)}dx'^0 \ . \tag{36}$$

Using Eqs. (35) and (36), we can compare the observed frequency ω_o from the surface of the star with that of the photon emitted from ∞ to the star, ω_e.

The proper time between crests (multiplied by c) gives the wavelength of the light or the reciprocal of the frequency. Therefore, using Eqs. (35) and (36), respectively, we obtain the following relationship [9]

$$\frac{\omega_o}{\omega_e} = \frac{d\tau_a}{d\tau_{a'}} = \frac{dx'^0}{dx^0} = \left(\frac{g_{00}(R)}{g_{00}(\infty)}\right)^{1/2} \ . \tag{37}$$

As measured by the observer at infinity, the photon coming from the surface of the star will have a frequency of

$$\omega_o = \mathrm{e}^{2\nu}\omega_e = \left(1 - \frac{2M}{R}\right)^\gamma \omega_e \ , \tag{38}$$

where in geometric normalized units, $G = 1$. The ratio ω_o/ω_e is given by

$$\frac{\omega_o}{\omega_e} = \left(1 - \frac{2M}{R}\right)^{\gamma/2} \ . \tag{39}$$

From Eq. (38), one can see that the photon arriving from the surface of the star to ∞ has a lower frequency than the photon arriving from ∞ to the surface of the star. The light is therefore red-shifted.

Conventionally, the gravitational redshift is defined by the fractional change between the observed and emitted wavelengths divided by the emitted wavelength [9]

$$z = \frac{\lambda_o - \lambda_e}{\lambda_e} = \frac{\lambda_o}{\lambda_e} - 1 = \frac{\omega_e}{\omega_o} - 1 \ . \tag{40}$$

Hence, using Eq. (40), we find the gravitational redshift to be

$$z = \frac{1}{\left(1 - \frac{2M}{R}\right)^{\gamma/2}} - 1 \ . \tag{41}$$

If $\gamma = 1$ then Eq. (41) will simplify for the spherical case as described by Eq. (19). By using the the mass and radii results shown in figures 10 and 11, we calculate the gravitational redshift z (Eq. (41)). The results are shown in figure 16.

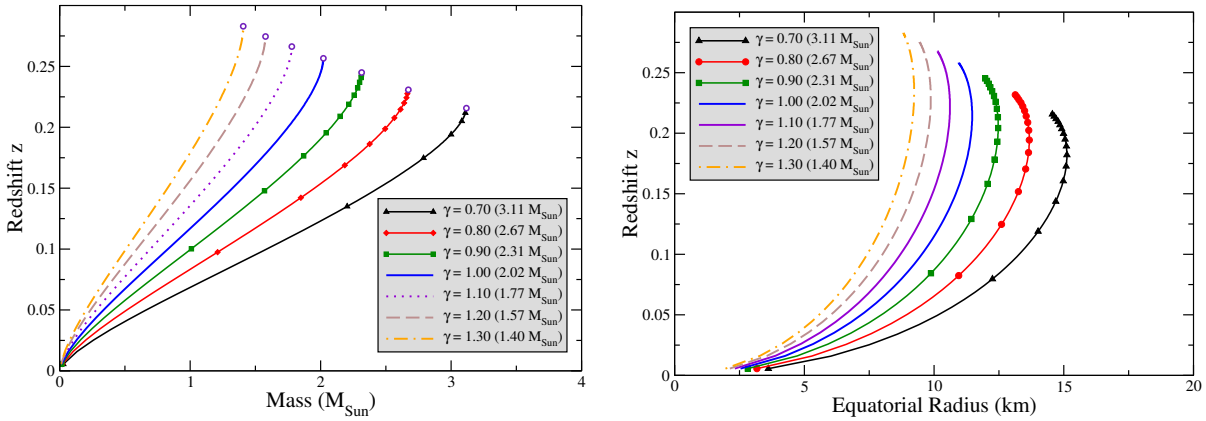

(a) (b)

Figure 16. (Color online) Calculated redshift values as function of mass and equatorial radii for various values of our deformation constant γ. (a) Redshift z as function of mass M. The circular dots represent the maximum mass from figures 10 and 11. (b) Redshift z as function of equatorial radii R.

Using the results in figure 16, one can directly calculate either mass or radii if the redshift z and either the mass or radii is known. Hence, we can use this numerical model for observational findings.

2.5. Conclusions

The goal of part 2 of this paper was to investigate the structure of deformed compact stars in the framework of general relativity and investigate how the deformation impacts the stellar properties of such objects. We have derived the stellar structure equations that govern the deformation. We have introduced a γ factor which we used to parameterize the deformation.

Having this parameterization allowed us to use a EoS in the limiting case of isotropy but still maintain deformation structure. From our results given in figures. 10 and 11, we see a slight change in deformation results in significant changes in mass and radii, and therefore we can conclude that the deformation does not need to be high to see these changes.

These promising results leads us to continue this work in the case of anisotropic EoS. However, for this case, we can not simply use a 1-D model governed by some deformation constant. We must have distinct hydro-static equations in both the radial and polar directions (i.e. dP/dr and dP/dz). This implies that we need to construct a full 2-D model of the global structure of our compact objects in this framework. Having a 2-D model will result in a more accurate representation of the deformation and therefore obtain more realistic calculations for stellar properties of these deformed compact stars.

3. Summary and Discussion

In this paper, we investigated two different solutions for compact stars in the framework of general relativity. In the first part of this paper, we solved Einstein's field equations for a non-vanishing cosmological and obtained a stellar structure equation in this framework. This structure equation has been suggested by a few authors already, but with inconsistent results.

From our results from figures 1 to 6, we see that in a Universe where the cosmological constant is very small, there is no significant contributions to the bulk properties such as mass and radius.

In the second part of this paper, we examined the deformation of compact stars. We introduced a deformation constant γ and a parameterization of the polar coordinate to obtain a 1-D description of the stellar structure of these deformed compact objects. We can conclude from figures 10 and 11 that slight change in deformation results in appreciable masses, and hence, the deformation does not need to be high to see significant mass changes.

Acknowledgments

This work is supported through the National Science Foundation under grants PHY-1411708 and DUE-1259951. Additional computing resources are provided by the Computational Science Research Center and the Department of Physics at San Diego State University. The research reported in this publication is also supported by the National Institute of General Medical Sciences of the National Institutes of Health under award number 5T34GM008303-25.

The authors would like to thank Vivian de la Incera and Efrain Ferrer from The University of Texas at El Paso, for their insightful discussions and initial motivation on this work. The authors would also like to thank Dr. James O'Brien for the invitation to speak at the biannual 2014 IARD conference.

The content is solely the responsibility of the authors and does not necessarily represent the official views of the National Institutes of Health.

References

[1] Perlmutter S et al 1999 *Astrophys. J.* **517** 565-86.
[2] Riess A G et al 1988 *Astron. J.* **116** 1009-38.
[3] Oppenheimer J R and Volkoff G M 1939 *Phys. Rev.* **55** 374-81.
[4] Tolman R C 1939 *Phys. Rev.* **55** 364-73.
[5] Vinayaraj O K and Kuriakose V C 2008 *arXiv: 0802.1155v2* [astro-ph].
[6] Ghezzi C R 2011 *Ap & SS* **333** 437-47.
[7] Silbar R and Reddy S 2004 *Am. J. Phys.* **72** 892-905.
[8] Zubairi O and Weber F 2014 *Astron. Nachr.* **335** 593-98.
[9] Glendenning N K 1997 *Compact Stars: Nuclear Physics, Particle Physics, and General Relativity* (New York: Springer-Verlag) P 7-123.
[10] Weber F 1999 *Pulsars as Astrophysical Laboratories for Nuclear and Particle Physics* (London: IoP Publishing) P 311-357.
[11] Carroll S M 2001 *Living Rev. Relativity* **3** 1.
[12] Chodos A, Jaffe R L, Johnson K, Thorn C B, and Weisskopf V F 1974a *Phys. Rev. D.* **9** 3471-95.
[13] Chodos A, Jaffe R L, Johnson K, and Thorn C B, 1974b *Phys. Rev. D.* **10** 2599-2604.
[14] Farhi E and Jaffe R L 1984 *Phys. Rev. D.* **30** 2379.
[15] Weber F 2005 *Progress in Particle and Nuclear Physics* **54** 193-288.
[16] Weber F 2003 *Nucl. Phys.* **721** 1032c-35c.
[17] Alcock C, Farhi E, and Olinto A 1986 *Astrophys. J.* **310** 261-72.
[18] Alcock C and Olinto A 1988 *Ann. Rev. Nucl. Part. Sci.* **38** 161-84.
[19] Witten E 1984 *Phys. Rev. D.* **30** 272-85.
[20] Glendenning N K, Kettner Ch., and Weber F. 1995 *Astrophys. J.* **450** 253-61.
[21] Tegmark M et al 2004 *Phys. Rev. D.* **69** 103501.
[22] Ferrer E, Incera V, Keith J, Portillo I, and Springsteen P 2010 *Phys. Rev. C.* **82** 6.
[23] Weyl H. 1918 *Ann. Phys.* (Leipzig), **54** 117.
[24] Zubairi O, Spinella W, Mellinger R, Weber F, Osaria M, and Contrera G 2014. In preparation
[25] Herrera L Filipe M, and Santos N O, 1999 *J. Math Phys.* **40** 8.
[26] Esposito F and Witten L 1975 *Phys. Lett.* **58B** 357.